Generalized multistability and noise-induced jumps in a nonlinear dynamical system

F. T. Arecchi,* R. Badii,[†] and A. Politi

Istituto Nazionale di Ottica, Largo Enrico Fermi 6, 50125 Firenze, Italy

(Received 4 April 1985)

A study of the forced Duffing equation is reported, with particular reference to a region of the parameter space where five different attractors coexist. This coexistence, reported in some recent experiments, is called generalized multistability. The role of external noise in bridging the otherwise disjoint basins is explored. Noise-induced couplings are shown to be ruled by simple kinetic equations under a general assumption for the geometry of the boundaries. These kinetic equations yield low-frequency power spectra in qualitative agreement with the experimental results.

I. INTRODUCTION—THE DUFFING OSCILLATOR

In the last few years many papers have dealt with the transition from order to chaos in dissipative dynamical systems.[1] Three routes to chaos (period doubling, intermittency and quasiperiodicity) have been extensively studied as possible "scenarios"[2] chosen by a nonlinear system to eventually land into a strange attractor, and the ways a strange attractor loses its stability (crises) have been investigated.[3]

Here we study another, rather general, characteristic of dynamical systems, namely, the coexistence of many different attractors for the same control parameters. We have called this property "generalized multistability",[4,5] in order to distinguish it from the ordinary coexistence of stationary solutions. The relevance of the coexistence of infinitely many periodic unstable solutions is by now sufficiently clarified and taken as synonymous of a deterministic chaotic motion. In such cases, the role of an additional random noise is not relevant since the structure of a strange attractor is not substantially modified.

On the contrary, not much attention has been given by physicists to the possible coexistence of infinitely many periodic stable solutions, as was conjectured by Newhouse.[6] We report the core of his conjecture from Ref. 7: ". . . in the parameter range where the horseshoe[8] is in the process of creation, an infinite number of families of stable periodic orbits are created." The region of coexistence of these many stable orbits is a critical one, since a small noise may switch the physical system from one orbit to any other, adding a new feature to usual chaotic scenarios. Such a coexistence was numerically explored by Ueda[9] without, however, attempting to evaluate the transition rates.

A qualitative hint on the role of multiple basins of attraction is contained in some experimental observations of hydrodynamic[10,11] instabilities.

Clear evidence of generalized multistability was first shown in an electronic oscillator[12] and then in a modulated laser system.[4] In both cases, the appearance of different attractors in phase space was associated with a low-frequency spectral component due to noise-induced jumps among different attractors. Both measurements, however, might be considered as experimental artifacts. In fact other systems show evidence of single attractors made of two subregions with infrequent passages from one to the other (see, e.g., the Lorenz attractor[13]). In such cases the low-frequency tail corresponds to the sporadic passages (deterministic diffusion),[14,15] and it does not require added noise. Therefore measurements of the power spectra are insufficient to discriminate between the two phenomena, and we must in addition specify the role of noise.

The noise-induced couplings have been studied so far in a simplified model, namely a cubic recursive map, allowing for two simultaneous attractors plus a long transient bridging the two solutions.[16] Here we present a numerical study of differential systems, that is, the forced Duffing oscillator with a double-well potential,

$$\ddot{x} + \gamma \dot{x} - x + 4x^3 = A\cos(\omega t) . \tag{1}$$

Many relevant features of this oscillator have been studied by Holmes and a thorough report can be found in Ref. 7.

Before entering into details, we realize already that two limit cycles can coexist for the same control parameters (A, ω), thus showing a simple example of generalized bistability. It is indeed well known that the amplitude response curve versus the frequency of the forcing term of a nonlinear oscillator is a curve bent as in Fig. 1, thus yielding a hysteresis phenomenon (bistability).[17] This means that, even inside a single potential well, two stable periodic solutions can coexist.

Dynamical systems with more than one final state have a highly complex interlacing of basins of attraction. In general the basins boundaries are not simple curves but, instead, their fractal dimension[18] is usually larger than 1, that is, there exist infinitely many points in the phase space whose neighborhoods (of radius ϵ) arbitrarily contain many points belonging to different basins of attraction for any ϵ value.

In Sec. II we present a numerical study of a limited region of the parameter space (A, ω) with particular reference to a fixed set of parameter values, where five attractors simultaneously coexist. In the Appendix the structure of a particular basin of attraction is studied in detail.
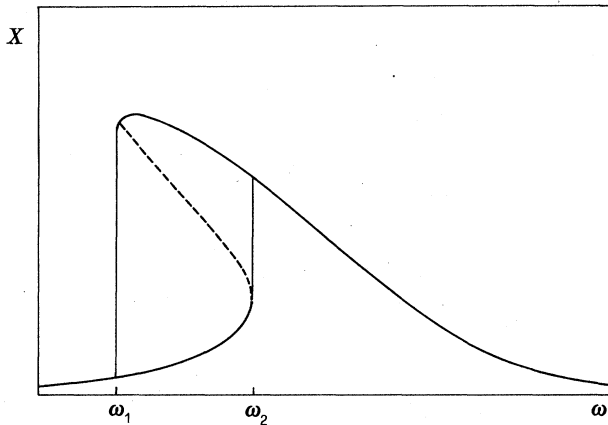
FIG. 1. Generic response curve $X(\omega)$ for a nonlinear damped oscillator vs the forcing frequency and for a fixed value of the external force. The values ω_1 and ω_2 indicate the boundaries of the hysteresis region.

In Sec. III we discuss the role of external noise in jumping from one attractor to the other, evaluating the escape times and the reinjection probabilities, thus yielding the necessary information for evaluating the power spectra.

II. THE PARAMETER SPACE

Numerical study of Eq. (1), performed for limited ranges of the external parameters A and ω, and for fixed $\gamma = 0.154$, yields many coexisting periodic islands. They correspond to attractors whose Poincaré section is made of a finite number N of points and hence they have a period N times that of the external force (Nth subharmonic).

The Poincaré section is built by plotting both x and $\dot{x}$ any time the phase of the external crosses a preassigned value. Each period N attractor arises by tangent bifurcation.[19] As the control parameters drive the system toward chaos, each of the N points of the Poincaré section generates a new one in its neighborhood, up to when we have N disconnected chaotic region, each one made of a Cantorlike set. For instance, if we start from period 3, each of the three points of the Poincaré section gives rise to a neighborhood of 2^k points at the kth bifurcation, but the three neighborhoods are still located around the initial positions and they are visited sequentially so that they can be considered as a perturbed period 3 even in the chaotic limit, where the number of points in each cluster is no longer finite. Since, starting from a period-N attractor, we can follow its N subregions up to the chaotic limit, we call "period N" that region of parameter space that includes both the strictly periodic solutions characterized by N points, as well as the chaotic ones characterized by N subregions sequentially visited. Only when, through a crisis, the N regions merge together, the attractor loses its individuality and we speak of death of the period-N attractor.

In Fig. 2 the contours of the stability regions for some of these attractors have been drawn and the respective periodicity indicated by the attached numbers.
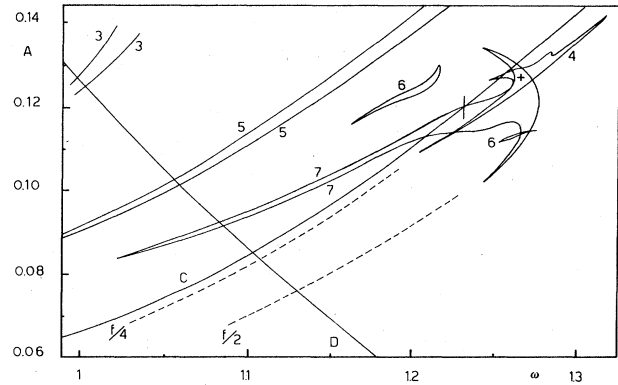

FIG. 2. Phase diagram of the Duffing equation showing the type of solutions for each pair of driving parameters (A,ω). The borderlines are the frontiers of the parameter regions corresponding to ordered motion, and the associated numbers denote the periodicity. Curves C and D show the upper limit (in the amplitude A) for the stability region of solutions confined in one valley. The vertical bar at $\omega = 1.22$ indicates the region where the escape times have been measured.

The meaning of the lines C and D is understood by referring to the two valleys of the potential of Eq. (1). Line C is a borderline above which there are no longer stable solutions confined in one valley. Below line C there is a manifold of lines, approximately parallel to it, which corresponds to a sequence of period doubling bifurcations and with mutual distances ruled by the Feigenbaum δ. These have been omitted for clarity reasons. They have already been observed experimentally (see Fig. 1 of Ref. 20) in an electronic oscillator ruled by Eq. (1); which is, however, affected by too large a noise to display the other interesting details reported in Fig. 2.

On the left of line D, there is a small limit cycle confined in one valley. This limit cycle does not undergo subharmonic bifurcations and it dies via tangent bifurcations, crossing line D.

Hence in the triangular region below the two lines C and D there is the coexistence of the small limit cycle with another one belonging to the above-mentioned Feigenbaum cascade.

The interplay between the two attractors can be appreciated if we draw the oscillator response versus the driving frequency at constant amplitude A, (moving horizontally in Fig. 2). A qualitative sketch of such a response has been already given in Fig. 1, where we see that two stable branches may coexist for $\omega_1 < \omega < \omega_2$. More precisely, at $\omega = \omega_2$ (ω_1), the smallest (largest) limit cycle disappears, yielding a point of line D (C) of Fig. 2. It is important to recall that the response curve shown in Fig. 1 is evaluated by means of perturbative techniques[17] that converge only for small amplitude solutions, when the nonlinear terms can be suitably taken into account. This may not be the case for the upper branch solution that visits highly anharmonic regions. Indeed, Fig. 1 describes only the disappearance of the large response solution, without any reference to subharmonic bifurcations, first observed in Ref. 21.

Let us return to Fig. 2 and focus our attention to the

two period-6 regions: they correspond to different attractors both extended over the two potential valleys and accompanied by the respective symmetric ones. Indeed, if $x(t)$ is a solution of Eq. (1), it is readily seen that also $-x(t)$ is a solution, with the only difference being a shift of π relative to the phase of the forcing term. Hence the symmetry properties immediately tell us that any asymmetric attractor (as the period 4 and the two period 6 ones) is accompanied by its mirrorlike image.

We have discussed a very small part of the parameter space, but it is already so rich of relevant details that the rest of the paper will be confined to discuss the phenomena occurring in pieces of Fig. 2.

In the region denoted by a cross in Fig. 2 we have the coexistence of five attractors, namely, two period 4, one period 7, and finally, two period 2. Their basins of attraction (BA) are sketched in Figs. 3—5; namely, Fig. 3(a) and 3(b) refer to the two period-2 attractors, Fig. 4 to one of the two period 4 (the other is not given for simplicity), and Fig. 5 to the single period 7. The construction of the different BA's requires, in principle, the knowledge of their boundaries, that is, of the unstable manifold of suitable saddle points. However, such curves are so interlaced that it is practically impossible to draw a globally accurate picture. Thus we have preferred to follow a more direct approach, while leaving to the Appendix partial application of the formal method.
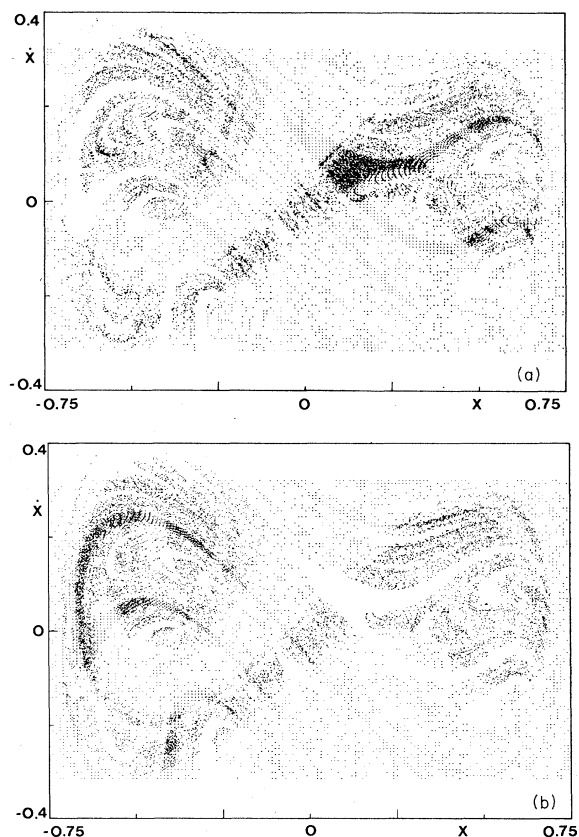
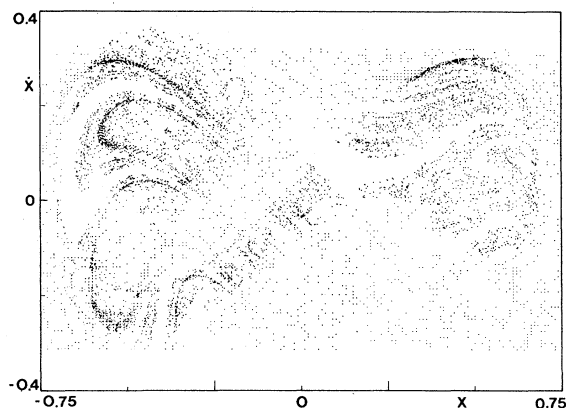We start from a uniform grid of 150×100 points in a

FIG. 4. Basin of attraction of one period-4 solution for the same values of A and ω as in Fig. 3.

Poincaré section with the phase of the external force put equal to 0. The x coordinates are distributed in the interval $(-0.75, 0.75)$ while the velocities stay within $(-0.4, 0.4)$. Each point of the grid, considered as the initial condition for Eq. (1), generates a trajectory that asymptotically falls in one of five coexisting attractors. Every initial point is consequently associated with the basin of attraction of the respective asymptotic solution (Figs. 3—5). Notwithstanding the mirrorlike symmetry between even-period limit cycles, their basins of attraction do not exhibit any symmetry [compare Figs. 3(a) and 3(b)]. Indeed, solutions of Eq. (1) are invariant not under the reflection $(x,\dot{x}) \rightarrow (-x, -\dot{x})$ only, but if further one shifts the phase of the forcing term by π.

Furthermore, to give a better feeling for each basin of attraction, we have reported, together with each point of the initial grid, the next two iterates on the Poincaré section. Referring, for instance, to Fig. 5, we notice seven dense regions, showing the fast contraction rate towards the seven-point attractor.

Figures 6(a) and 6(b) are magnified versions of the central parts (around the origin) of Figs. 3(a) and (5), respectively, for an x interval $(-0.09, 0.09)$ and an $\dot{x}$ interval $(-0.06, 0.06)$. The superposition of the two graphs gives an idea of the intimate interlacing of the different BA's,

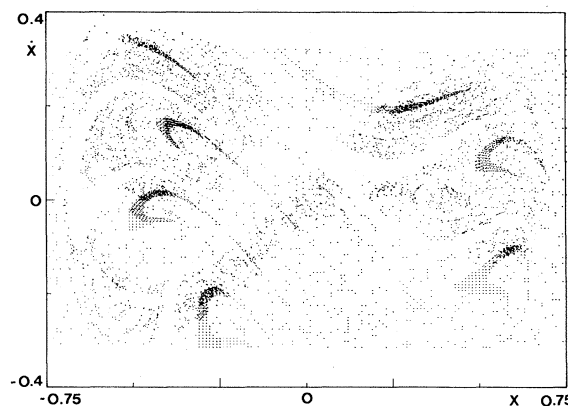FIG. 3. Basins of attraction of the two period-2 solutions for $A = 0.117$ and $\omega = 1.17$.

FIG. 5. Basin of attraction of the period-7 solution, taken in the same conditions as the previous figures.
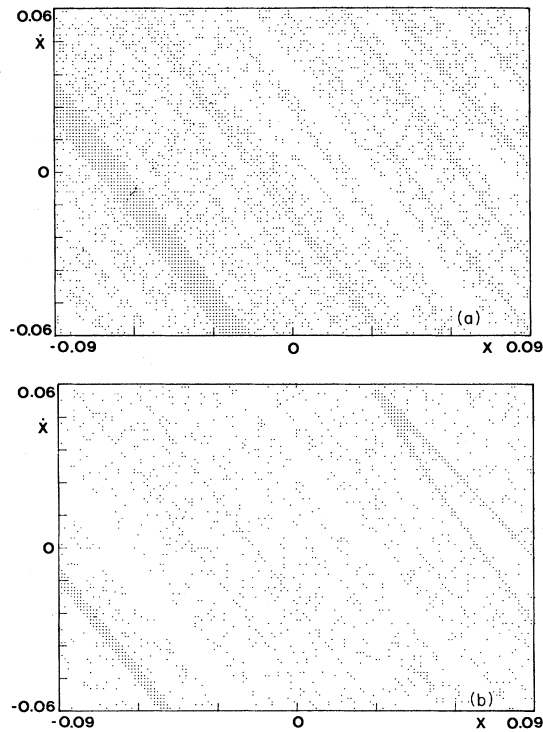
FIG. 6. Expansion of the central part of Fig. 3(a) (period-2 attractor) (a), and of Fig. 5 (period-7 attractor) (b).

thus showing how a tiny displacement in the initial condition may imply a change of the asymptotic solution, as shown recently by Grebogi et al.,[18] who have given evidence of the fractal nature of the border of a BA in a two-dimensional iteration map with two distant attractors. The same task for a differential equation is much more difficult, however a comparison between Fig. 6 and the previous Fig. 3, shows how an improvement by a factor of 8 in the definition of the initial grid does not permit a clear-cut discrimination among the BA's.

III. ROLE OF EXTERNAL NOISE—LOW-FREQUENCY SPECTRA

In the previous section we have considered the noise-free dynamical system, focusing our attention on the occurrence of different asymptotic solutions and on the structure of their BA's. Now, by adding an external white noise in Eq. (1), jumps among different attractors become possible. Such a phenomenon is particularly evident close to the marginal stability points of the attractors, when the occurrence of even very small noise spikes is sufficient to let the point leave the attractor. In the standard multistability (coexistence of different fixed points) marginal stability means that we are near a tangent bifurcation. In this case of generalized multistability another class of critical phenomena must be considered, namely the crisis.[3]

Indeed, the distance of the attractor's support from the border of its BA is equal to zero both for a tangent bifurcation and for a crisis. However, in the former case the BA itself shrinks to zero, whereas in the latter case it is

the attractor that spreads up to the border of its BA.

As for the intermittency,[22] we can introduce a relevant parameter to describe a noise-induced crisis, that is, the mean escape time T from the attractor. Such a parameter has been proved[5] to depend, through a universal scaling law, on the noise-amplitude σ and on the distance from the crisis value ϵ.

$$T = \sigma^\alpha F(\epsilon/\sigma^\beta) \, . \tag{2}$$

For the case of a logistic map the exponents are (Ref. 5) $\alpha = -\frac{1}{2}$ and $\beta = 1$.

Indeed, referring to the logistic map and for a Gaussian noise, the time T is

$$T = \pi\sqrt{2/\sigma}e^{\epsilon^2/\sigma^2}/D_{-3/2}(\epsilon/\sigma) \, , \tag{3}$$

where D is the parabolic cylinder function.

Quite below crisis, for $\epsilon \gg \sigma$, the main dependence of T on the noise amplitude is an exponential one

$$T = \frac{\pi}{\sqrt{2}} \frac{\epsilon^{3/2}}{\sigma^2} e^{\epsilon^2/2\sigma^2} \, , \tag{4}$$

very similar to the Kramers diffusion law.[23] Here, however, the physics is wholly different. Let us consider the small noise limit in order to make a sensible comparison with Kramers's approach. In our case the density of points on the attractor is generated by the deterministic equations and is barely affected by the small noise. In contrast in Kramers's problem, the probability density within the potential valleys is essentially determined by the applied noise as in any Langevin problem.

Even though the above relations (3) and (4) have been derived for discrete maps, we can reasonably assume that the same qualitative behavior has to be expected also for a differential equation. In fact for the Duffing equation (1), we have studied the dependence of the mean escape time on the noise amplitude for different values of the external force (see vertical bar in Fig. 2), moving from below to above the crisis of the period-7 attractor. Specifically, at each integration step (which was $\frac{1}{100}$ of the forcing period) $\dot{x}$ has been shifted by a random number selected from a Gaussian distribution with zero mean and rms σ. Due to the smallness of the integration step, such a procedure is a good approximation of a white Gaussian noise. The results are plotted in Fig. 7. For amplitude values below the crisis, the exponential growth clearly appears and, moreover, approaching the marginal stability point, the rate of change of T shows a slowing down that eventually leads to a saturation above the crisis value $A = A_\epsilon$. Indeed, for $A > A_c$, the attractor looses its stability and even without noise it jumps out of its previous BA. So far we have discussed the escape from an attractor. If we want to complete the description of the jumps among the attractors, we need also some information on the reinjection probabilities. The escape problem requires knowledge of the pseudo-invariant distribution of any single attractor and the distance from the border of its BA; the reinjection deals with the interlacing of the different BA's and it is clearly connected with their respective areas.

As we have seen in Sec. II, all the BA's are interlaced over infinitely small length scales, and this makes possible
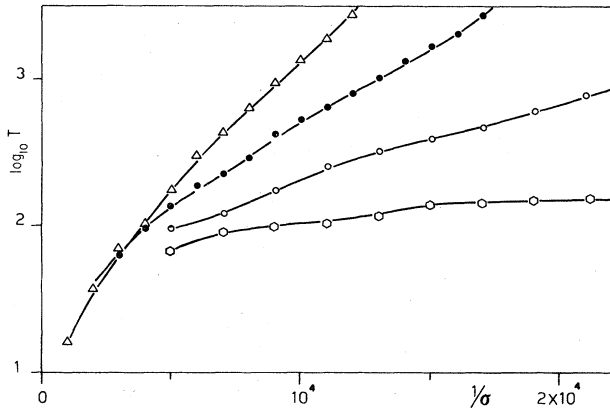
FIG. 7. Mean escape time for the period-7 region vs the inverse of the noise amplitude. All the curves refer to the same frequency, but with different A's. Namely, the symbols $\triangle$, $\bullet$, $\circ$, $\circ$ represent, respectively, $A = 0.1170$, 0.1171, 0.1172, and 0.1173 ($\geq A_c$).

a probability analysis of the reinjections because any attractor may be within reach (via a jump induced by a suitable noise amplitude) from a larger number of BA's that are surrounding the attractor itself.

Let us then refer to a generic situation with m simultaneously coexisting attractors and call $p_i(t)$ the instantaneous probability to be on the ith attractor. According to the previous assumption, the rate equation for p_i is

$$\dot{p}_i = -a_i p_i + \sum_{j=1}^{m} s_{ij} a_j p_j , \qquad (5)$$

where a_i is the inverse of the mean escape time $(1/T)$ from the ith attractor and s_{ij} is the jump probability from the jth attractor onto the ith one, and is grossly given by the area of the ith BA spanned from any point of the attractor by a leap of the noise amplitude order.

Two terms containing p_i are present in the right-hand side of Eq. (5). Indeed, besides $-a_i p_i$, which is the escape rate from the ith attractor, $+s_{ii} a_i p_i$ takes into account the occurrence of an immediate reinjection. This leads to a distinction between the mean escape time $T = 1/a_i$ and the residence time that is increased by jumps from the attractor onto itself. Such a distinction is meaningful when the transients the system takes to "decide" which attractor to land on,[24] are very short compared to T. This is indeed the case we have analyzed ($\omega = 1.22$, $A = 0.114$) with two period-2 and one period-7 attractor. Whenever such transients become very long, it is still possible to describe the evolution by means of equations like Eq. (5), but the transient has to be considered as another region (like those occupied by attractors) that bridges all the multistable solutions together without any other direct coupling. An example of such a behavior has been described in Ref. 16 where, in a one-dimensional cubic map, two period-3 attractors were coupled only through a long transient.

The logical schemes referring to the two different conditions (Duffing with three attractors and cubic map) have been sketched in Fig. 8.

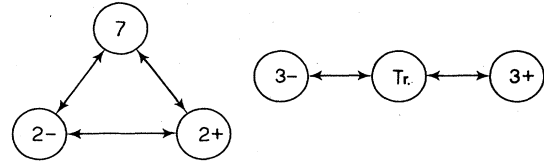As shown in Ref. 16, solution of kinetic equations al-

FIG. 8. Logical schemes showing the possible coupling among the attractors in two different cases: (a) Duffing equation with the three attractors (one period 7 and two period 2); (b) one-dimensional antisymmetric cubic map with two period-3 attractors plus a long transient (T).

lows the evaluation of the correlation function and hence, under the general assumptions listed in that reference and plausible in the present case, evaluation of the stationary power spectrum. Calling $x = x(t)$ and $x' = x(t + \tau)$, the correlation function of the dynamical process is defined as the ensemble average over the joint probability distribution $p(x)p(x \mid x')$ of the two events, that is,

$$R(t, t + \tau) = \int dx \int dx' x x' p(x) p(x \mid x') \qquad (6)$$

and the averaged correlation function can be written as

$$\langle R(\tau) \rangle = \lim_{\bar{t} \to \infty} \frac{1}{2T} \int_{-\bar{t}}^{\bar{t}} R(t, t + \tau) dt . \qquad (7)$$

As said previously, the motions within each attractor can be taken as decorrelated from the jumps as well as decorrelated from one to another attractor. Therefore, the time average yields either the correlation function $\langle x_i x_i(\tau) \rangle$ or just $\langle x_i \rangle \langle x_j \rangle$ for $i \neq j$, where x_i coincides with $x(t)$ onto the ith attractor and is 0 elsewhere; analogously the probabilities $p(x), p(x \mid x')$ reduce the the jump probabilities p_i and $p_j(\tau, i)$. These latter ones are those solutions of Eq. (5) taken with the following criteria: $p_j(\tau, i)$ is the conditional probability of j at time τ, when $p_i = 1$ at $\tau = 0$; p_i is the asymptotic probability of i for $\tau \to \infty$, independent of the initial condition. With such assumptions, the above correlation function becomes

$$\langle R(\tau) \rangle = \sum_i \langle x_i x_j(\tau) \rangle p_i p_j(\tau, i)$$

$$+ \sum_{i \neq j} \langle x_i \rangle \langle x_j \rangle p_i p_j(\tau, i) . \qquad (8)$$

Neglecting the oscillating terms of $\langle x_i x_j(\tau) \rangle$, which contribute to the high-frequency spectrum, and besides a zero-frequency component, the low-frequency spectrum is made in general of $m - 1$ Lorentzians, plus a background corresponding to the fast mixing within the transient region.

We have thus shown that the simultaneous coexistence of m attractors leads in general to a power spectrum made of $m - 1$ Lorentzians. Symmetries in the attractors may reduce the number of independent coefficients and hence the number of Lorentzians that make the spectrum. This can be particularly relevant for fitting a limited region of the low-frequency spectrum with a power law $S(f) = f^{-\alpha}$ as discussed in Refs. 12 and 16.

We specify the above arguments with the numerical results obtained for $A = 0.114$ and $\omega = 1.22$. For an external noise rms equal to 2.5×10^{-4}, the mean escape times
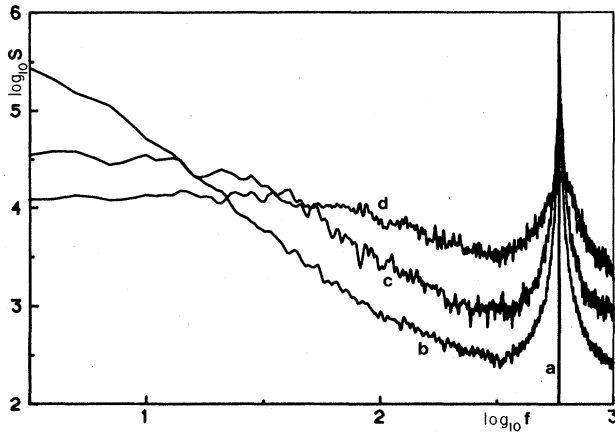
FIG. 9. Power spectrum for the Duffing oscillator for $A = 0.114$, $A = 1.22$ and for different external noise levels the following: (a) 2.5×10^{-5}, (b) 2.5×10^{-4}, (c) 5.0×10^{-4}, (d) 2.0×10^{-3}. The peak on the right corresponds to $f = 1.22/14$ and comes from the period-7 attractor.

from the period-7 attractor and the two period-2 attractors are, respectively, 158 ± 10 and 180 ± 10 (the period of the forcing term being the time unity), while the mean residence times turn out to be 413 ± 20 and 206 ± 10. The large difference between the two averages referred to the period-7 attractor yields a large value for the reinjection probability s_{77} from such attractor back to itself, which is, indeed around 62%. Therefore, since $s_{77} + 2s_{27}$ has to be 1, s_{27} turns out to be 19% while the probability s_{22} of a jump back to the period 2 is lower, namely 12%. Incidentally, $s_{2\text{-}2}$ is very close to s_{22}, even if this is not imposed by the symmetry properties. Finally, again from the normalization condition $s_{22} + s_{-22} + s_{72} = 1$, s_{72} is 76%, hence even larger than the probability of a jump from the period-7 attractor back onto itself.

All of these data contribute to determine the power spectrum S of $x(t)$ shown in Fig. 9 (see curve b). A complete characterization of the low-frequency part is, however, not yet possible, since we should also add the contribution of jumps between two different period-7 solutions (see Sec. II) and the low-frequency component of the two other attractors $(2, -2)$. A qualitative analysis of Fig. 9 shows, anyhow, that, when increasing the noise level from 2.5×10^{-5} to 2.5×10^{-4}, 5.0×10^{-4} and 2.0×10^{-3} (respectively, curves a,b,c,d), the following sequence of events occurs: in a, no jumps occur during the measurement and the solution remains in the initial attractor (namely, a period-7 one); in b, a well-defined low-frequency contribution shows up and, finally, it broadens in c,d indicating faster decay rates.

IV. CONCLUSION

We have shown how addition of noise to deterministic chaos induces a low-frequency spectral component made in general by the superposition of $m - 1$ Lorentzians, m being the number of coexisting attractors that characterize a multistable region of the parameter space. On the contrary, the high-frequency spectrum describing the decay

of the correlations within each stable attractor is practically not affected by the noise.

APPENDIX: NUMERICAL CONSTRUCTION OF THE BASIN BOUNDARY OF A PERIODIC ATTRACTOR

Here we show as example, the boundaries of the period-7 attractor. The seventh iterate of the Poincaré map, is made of seven distinct fixed points. Each one of them corresponds to the same attractor except for being observed with a different phase. For simplicity we focused our attention on the lowest point on the right of Fig. 5 and reconstructed its BA in the vicinity of the point itself (see Fig. 10).

Since the period-7 attractor arises via a tangent bifurcation, it is accompanied by its unstable counterpart. This is for instance shown in Fig. 10, where S and U indicate, respectively, the stable and unstable solution.

The contour of the BA is simply defined by the stable manifold of U, and it is made of two distinct curves E and I, as it appears from Fig. 10. We now study the behavior of E and I in the regions P, Q, where they approach one another.

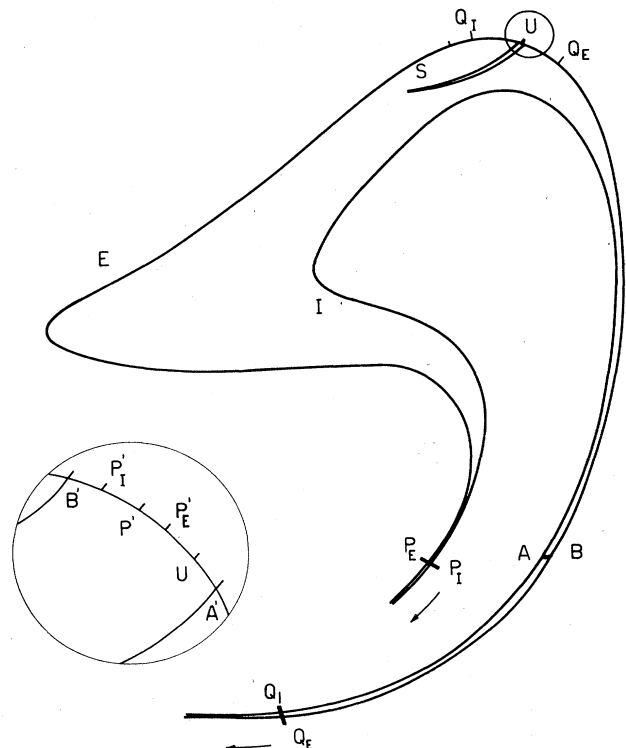We start by considering a transverse section of the basin

FIG. 10. Boundaries of the BA of the period-7 attractor around one of the points that make its Poincaré section, namely, the lowest one on the right of Fig. 1. S is the stable solution, while U indicates the unstable period 7 born together with the stable one via tangent bifurcation. E and I are the stable manifold of U. The expanded view around U is reported in the circle at the lower left and the role of the points P and Q is discussed in the text.

of attraction in the region P,Q. Let P_E (Q_E) and P_I (Q_I) be the end points of a section in region P (Q) belonging, respectively, to E and I. By iterating seven times P_E (Q_E) and P_I (Q_I), in order to have again the same phase, two new points P'_E (Q'_E) and P'_I (Q'_I) are generated.

If we specialize to the region P, P'_E and P'_I both fall at left of U. Moreover, when letting P_E and P_I move according to the arrow, P'_E and P'_I appear to converge towards the same point P'. Hence for continuity reasons, a point exists where E and I join together, perhaps forming a cusp.

The behavior of E and I is entirely different in the region Q. Indeed, the points Q'_E and Q'_I lie on E, but on opposite sides with respect to U and, moreover, the distance $Q'_E Q'_I$ increases when Q_E and Q_I move along the arrow. Therefore, the expansion rate $Q'_E Q'_I / Q_E Q_I$ seems to diverge because $Q'_E Q'_I$ increases as $Q_E Q_I$ decreases.

However, we can reasonably suppose that, moving forward Q_E and Q_I, the distance $Q'_E Q'_I$, starts decreasing after having reached a maximum value, thus solving the apparent paradoxical result.

This phenomenology is shared by the other six subregions of the period-7 attractor, and it seems to be a rather common feature. The phase plane $x,\dot{x}$ is, therefore, decomposable into a finite number of filamentous regions that are infinitely interlaced. This is a characteristic of complex dynamical systems that causes a high sensitivity to initial conditions in the sense of Ref. 18.

Finally, in order to show the stretching and folding properties of the seventh iterate of the Poincaré map, we have drawn the image of a transversal segment AB. Both the iterates A' and B' of A and B fall in the neighborhood of U, while the interior of AB extends from U towards S as shown in Fig. 10.

---

[*]Also at Dipartimento di Fisica, Università di Firenze, Italy.

[†]Present address: Physik Institut der Universitat, Zurich 8001, Switzerland.

[1]Due to the vast amount of papers on the subject, we report here, for simplicity, the proceedings of some recent conferences or school on this subject, namely Chaotic Behavior in Dynamical Systems, edited by G. Iooss and R. H. G. Helleman (North-Holland, Amsterdam 1983); Order in Chaos, proceedings of the Los Alamos Conference, Los Alamos, New Mexico, 1982 [Physica 7D, 3 (1983)]; N. B. Abraham, J. Gollub, and H. Swinney, Review of Haverford Workshop, Haverford, 1983 [Physica 11D, 252 (1984)].

[2]J. P. Eckmann, Rev. Mod. Phys. 58, 643 (1981).

[3]C. Grebogi, E. Ott, and J. A. Yorke, Phys. Rev. Lett. 48, 1507 (1982).

[4]F. T. Arecchi, R. Meucci, G. Puccioni, and J. Tredicce, Phys. Rev. Lett. 49, 1217 (1982).

[5]F. T. Arecchi, R. Badii, and P. Politi, Phys. Lett. A 103, 3 (1984).

[6]S. E. Newhouse, Topology 13, 9 (1974).

[7]J. Guckenheimer and P. Holmes, Nonlinear Oscillation, Dynamical Systems, and Bifurcations of Vector Fields (Springer, Berlin, 1983).

[8]S. Smale, Differential and Combinatorial Topology, edited by S. S. Cairns (Princeton University, Princeton, N.J., 1963).

[9]Y. Ueda, Report No. IPPJ-430, Nagoya University, 1979 (unpublished).

[10]J. Maurer and A. Libchaber, J. Phys. (Paris) Lett. 41, 515 (1980).

[11]M. Giglio, S. Musazzi, and U. Perini, Phys. Rev. Lett. 47, 243 (1981).

[12]F. T. Arecchi and F. Lisi, Phys. Rev. Lett. 49, 94 (1982); 50, 1328 (1983).

[13]C. Sparrow, The Lorenz Equation (Springer, Berlin, 1982).

[14]T. Geisel and J. Nierwetberg, Phys. Rev. Lett. 48, 7 (1982).

[15]D. D'Humieres, M. R. Beasley, B. A. Huberman, and A. Libchaber, Phys. Rev. A 26, 3483 (1982).

[16]F. T. Arecchi, R. Badii, and A. Politi, Phys. Rev. A 29, 1006 (1984).

[17]P. Hagedorn, Nonlinear Oscillations (Clarendon, Oxford, 1982).

[18]C. Grebogi, S. W. McDonald, E. Ott, and J. A. Yorke, Phys. Lett. A 99, 415 (1983).

[19]P. Collet and J. P. Eckmann, Iterated Maps (Birkhauser, Boston, 1980).

[20]F. T. Arecchi and A. Califano, Phys. Lett. A 101, 443 (1984).

[21]B. A. Huberman and J. Crutchfield, Phys. Rev. Lett. 43, 1743 (1979).

[22]Y. Pomeau and P. Manneville, Commun. Math. Phys. 74, 189 (1980).

[23]H. A. Kramers, Physica (Utrecht) 7, 284 (1940).

[24]In general, the BA chosen by the first jump does not necessarily mean that the system will asymptotically go onto the corresponding attractor. Since noise is applied at each step, the point may leave the first BA and wander over other ones, depending on the width of the BA's themselves. This wandering is what we define as "transient."